
Original Articles

Cytometric Quantification of Nitrate Reductase by Immunolabeling in the Marine Diatom *Skeletonema costatum*

Frank J. Jochem,^{1*} G. Jason Smith,² Yu Gao,³ Richard C. Zimmerman,² Alejandro Cabello-Pasini,⁴ Donald G. Kohrs,² and Randall S. Alberte⁵

¹The University of Texas at Austin, Marine Science Institute, Port Aransas, Texas

²Moss Landing Marine Laboratories, Moss Landing, California

³Rutgers, The State University of New Jersey, New Brunswick, New Jersey

⁴Universidad Autonoma de Baja California, Ensenada, Mexico

⁵PhycoGen, Inc., Portland, Maine

Received 23 August 1999; Revision Received 22 November 1999; Accepted 24 November 1999

Background: The uptake of nitrate by phytoplankton is a central issue in biological oceanography due to its importance to primary production and vertical flux of biogenic carbon. Nitrate reductase catalyzes the first step of nitrate assimilation, the reduction of NO₃ to NO₂. A cytometric protocol to detect and quantify relative changes in nitrate reductase (NR) protein content of the marine centric diatom *Skeletonema costatum* is presented.

Methods: Immunolabeling of NR protein was achieved with polyclonal antibodies raised against *S. costatum* NR. Antisera specific to a NR protein subunit and to a NR polypeptide sequence were compared, and cytometric results of NR protein abundance were related to Western analyses. Changes in cellular NR abundance and activity were followed during an upwelling simulation experiment in which *S. costatum* was exposed to a shift from ammonia to nitrate as major nitrogen source.

Results: NR protein could be detected in NO₃-grown cells and at extremely low levels hardly discernible by Western

Blot densitometry in NH₄-grown cells. The protocol allowed observation of early stages of NR induction during an upwelling simulation. NR abundance increased after the nutrient shift to reach a new physiological “steady-state” 96 hrs later. NR activity exhibited diel variation with maxima at mid-day. NR abundance as estimated by both flow cytometry and Western analysis exhibited a hyperbolic relationship to NR activity. This pattern suggests post-translational activation of NR protein.

Conclusions: The presented protocol allows the differentiation of NH₄- versus NO₃-grown algae as well as the monitoring of early stages in the induction of nitrate assimilatory capacities. Cytometry 39:173–178, 2000.

© 2000 Wiley-Liss, Inc.

Key terms: *Skeletonema costatum*; flow cytometry; nitrate reductase; immunolabeling; upwelling; phytoplankton bloom

The uptake of nitrate by phytoplankton is a central issue in biological oceanography due to its importance to primary production and vertical flux of biogenic carbon. For an oceanic ecosystem, the rate of “new” production (relying on external inputs of nitrate in contrast to “regenerated” production thriving on ammonia; 1) directly relates to the sinking flux of biogenic material (2). Therefore, nitrate utilization rates should set the upper limit for carbon supply rates to benthic communities (3).

Assimilatory nitrate reductases (NR; EC 1.6.6.1) catalyze the first step of nitrate assimilation, the reduction of NO₃ to NO₂, in plants and fungi (4), thereby expend-

ing as much as 25% of photosynthesis-generated energy (5). A comprehensive understanding of intrinsic features of NO₃ metabolism in phytoplankton can yield substantial insights into the biological mechanisms underlying the dynamics of new production (6). Despite

Grant sponsor: German Research Council; Grant number: DFG Jo 192/5-5,6 to FJJ, Grant sponsor: Office of Naval Research to GJS, Grant sponsor: National Science Foundation to RCZ.

*Correspondence to: Frank J. Jochem, Marine Science Institute, 750 Channel View Drive, Port Aransas, TX 78373.

E-mail: frank@emcs.de

growing knowledge of NR activity in diverse phytoplankton (7) and attempts to correlate NR activity to algal growth rates and the environment's nitrogen condition (8, 9, 10), important aspects of NR regulation and control at the cellular and molecular level have not been addressed adequately (6, 11).

Attempts to provide mechanistic information on intrinsic processes driving NO_3 metabolism have been impeded due to technical difficulties in isolating and characterizing the key biochemical components (6). The present work describes an immunofluorescence-based cytometric protocol to detect and quantify changes in NR protein content in the marine centric diatom *Skeletonema costatum* and the application of this protocol to investigate the dynamics of NR protein and activity induction during changes in nitrogen source and supply rate. Additionally, the utility of flow cytometric analysis of NR protein abundance, as a proxy for nitrate assimilation capacity, is assessed. *S. costatum* was chosen due to its ecological importance; being a prominent bloom-forming species in diverse marine systems upon nitrate entrainment into the upper water column by upwelling, wind mixing or land runoff (12, 13).

MATERIALS AND METHODS

Skeletonema costatum (CCMP 1332) was cultured in 0.2 μm filtered and autoclaved Monterey Bay seawater with $f/2$ nutrients (14, 15) containing 62 μM NH_4 (60 μM added, 2 μM in natural seawater) and 22 μM NO_3 (from natural seawater). Light (200 μmol quanta m^{-2} s^{-1}) was provided under a 16:8 light/dark cycle.

For the simulated upwelling nitrogen-shift chemostat experiment, a 20 L polycarbonate carboy was inoculated with a one-liter culture (5×10^5 cells ml^{-1}) of *S. costatum* and medium was supplied at a dilution rate of 0.12 d^{-1} . This low f -ratio (i.e. the ratio of ammonia over total inorganic nitrogen concentration; 0.26) condition was maintained for 14 d prior to sampling at the mid-photocycle for 3 d prior to the N-source manipulation. At the onset of light (t_0), the medium supply was changed to high f -ratio (0.92; 2 μM NH_4 , 100 μM NO_3) and dilution rate (0.86 d^{-1}). The culture was sampled at 4 h intervals during the light and 2 h intervals during the dark periods for the following 5 d.

In vitro extractable NR activity was estimated from filtered cells that were frozen in liquid N_2 , resuspended in 0.1 M imidazole buffer (pH 7.5) containing 1 mM EDTA, 1 μM FAD, 5% (v/v) glycerol and protease inhibitors (120 μM Pefabloc, 20 μM leupeptin, 10 μg ml^{-1} chymostatin; all Sigma Chemicals, St. Louis, MO), and sonicated. The crude extracts were incubated in 0.1 M potassium phosphate buffer (pH 7.5) containing 1 mM EDTA, 100 μM NADH, 10 mM KNO_3 and 1 μM FAD for 30 min at 15°C. NO_2 formed during incubation was measured colorimetrically using 2% sulfanilamide in 4 N HCl and 0.2% N-1-naphthyl-ethylenediamine (NED; Sigma Chemicals) at 540 nm in a Hewlett-Packard 8452A diode array spectrophotometer.

Polyclonal antibodies against a *S. costatum* NR subunit were obtained as described in Gao et al. (11). Epitope-

specific antibodies were produced by injecting New Zealand White Rabbits with a synthetic peptide coupled to the KLH antigen and comprised of the sequence APAAKS-DRITA derived from the sequence of a 45 kDa V8 protease fragment of *S. costatum* NR. Both sets of crude antisera were enriched for NR-specific titer by affinity purification against the NR subunit polypeptide as described previously (11).

NR protein abundance was determined by standard Western analysis (16). Proteins in crude cell extracts were separated by SDS-PAGE and transferred electrophoretically onto nitrocellulose membranes by a BioRad (Hercules, CA) Mini Trans-Blot®. Non-specific protein binding sites on the membranes were blocked prior to antibody incubation by 2% Carnation non-fat dry milk in phosphate buffer saline (PBS, pH 7.4). NR subunit polypeptides were visualized by immunodecoration with an affinity-purified NR polyclonal Ig from *S. costatum* (11). Duplicate blots were digitized at 300 dots per inch (dpi) and 256 gray levels on an HPScanJet 4P. Densities of immunoreactive bands were quantified from the digitized images using the UTHSCSA ImageTool (V 1.25) software package (University of Texas Health Science Center, San Antonio, TX; freeware) by using non-immunoreactive regions of the membrane as the baseline intensity.

For whole cell immunofluorescence assays, cells were concentrated by centrifugation at 2500 g for 10 min at 15°C. Media was aspirated away from the cell pellet on ice, and the cells were flash fixed by resuspension in 96% ethanol at -20°C . After 24 h at -20°C , cells were concentrated by centrifugation, resuspended in fresh 96% ethanol at -20°C , and stored until processed for immunofluorescence. Prior to antibody labeling, cells were centrifuged and rinsed twice with a solution of 3% BSA in PBS. Non-specific binding sites were blocked in 3% BSA in PBS for 1 h on ice, and subsequent incubation with 2% DMSO (dimethylsulfoxide) in the blocking buffer for 30 min increased cell permeabilization. Cells were washed as above, resuspended in the BSA-PBS buffer containing the primary NR antibody at a 1:100 dilution (ca 1 μg μl^{-1}) and incubated for 1 h at room temperature. After washing 3 times with 0.05% Tween-20 in PBS, cells were resuspended in BSA-PBS buffer containing a 1:200 dilution of goat-anti-rabbit IgG-FITC conjugate (Sigma Chemicals) for 30 min at room temperature. Finally, all cells were washed with the PBS-Tween-20 buffer to remove unbound antibody complexes.

A parallel series of cells was treated only with the secondary antibody to control for background fluorescence and non-specific binding. Affinity purified antibody stocks for immunofluorescence assays were pre-absorbed with fixed *S. costatum* cells that had been grown with NH_4 as the sole nitrogen source in order to reduce the titer of non-NR-specific binding to cellular structures.

Cytometric analysis of 10,000 cells per sample was performed on a Becton Dickinson FACSort flow cytometer equipped with a 488 nm argon laser. *S. costatum* cells were identified and discriminated against (low amount of) debris in 2-parameter histograms of Forward

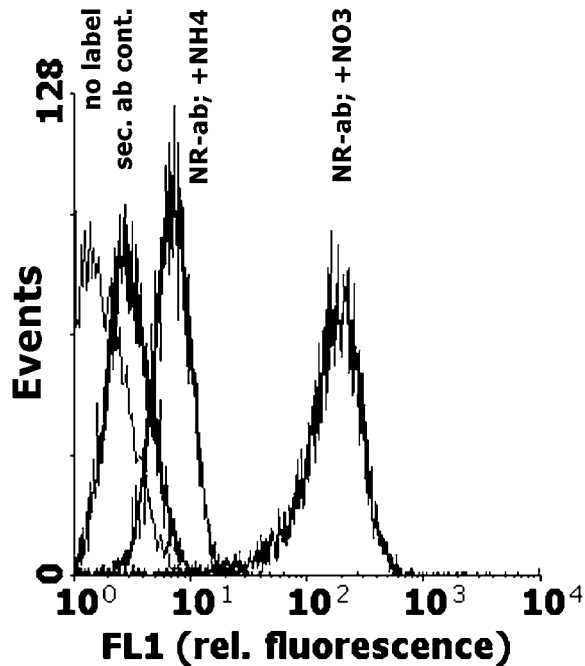


FIG. 1. Frequency histograms of green fluorescence (FL1, 530/30 nm) of *Skeletonema costatum* cells: after fixation (no label), with pre-immune rabbit antibodies control (sec.ab cont.), with anti-NR grown in NH_4 medium (NR-ab; + NH_4) and NO_3 -medium (NR-ab; + NO_3).

Angle Light Scatter (FSC) versus Side Angle Light Scatter (SSC). Green fluorescence of the FITC-conjugated secondary antibody was recorded through a 530/30 nm bandpass filter on a 1024 channels, 4 decades log scale, and the data were processed using WinList[®] software (Verity, Topsham, ME).

RESULTS AND DISCUSSION

Polyclonal NR protein subunit antiserum provided sufficient immunolabeling to detect NR protein in *Skeletonema costatum* grown under both nitrate and ammonia conditions. Although the protocol yielded some increase in fluorescence upon incubation with secondary Ig alone compared to untreated cells, treatment of NH_4 - and NO_3 -grown *S. costatum* with affinity purified anti-NR Ig followed by the secondary Ig resulted in sufficiently high and differential increases in FITC fluorescence (Fig. 1). The differences in fluorescence reflected differences in nitrate assimilation between these two cultures. The low NR contents under ammonia growth might be related to minor amounts of nitrate in the Monterey Bay water derived culture medium (see Materials and Methods), but low constitutive NR levels were reported in *S. costatum* grown on synthetic ammonia medium free of nitrate as well (17).

Comparison of different anti-NR immunoprobe stocks revealed a consistently higher fluorescence signal with the anti-NR subunit (S) as compared to the NR peptide (P, epitope-specific antibody), even when applied at the same Ig concentration (Fig. 2). This difference reflects the po-

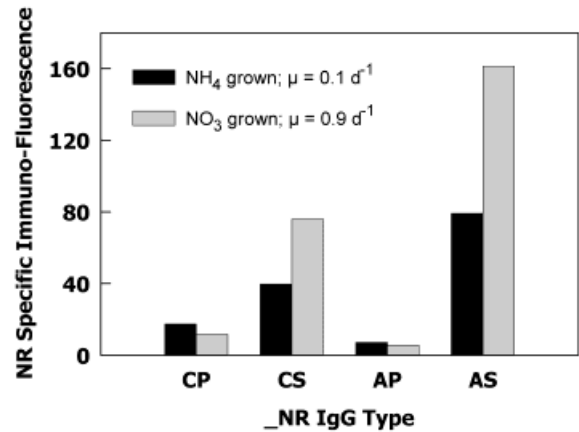


FIG. 2. NR specific fluorescence (mean values, relative units) of NH_4 - and NO_3 -grown *Skeletonema costatum* labeled by different protocols and antisera. C = crude affinity purified antiserum, A = affinity purified antiserum pre-sorbed to NH_4 -grown *S. costatum*, S = NR subunit probe, P = NR polypeptide sequence probe.

tentially greater number of epitopes accessible to the Ig pool generated against the entire NR subunit and suggests that, for low abundance targets like NR protein, multivalent Ig pools are better than single epitope targeted Ig. Pre-absorption of anti-NR protein Ig stocks with NH_4 -grown *S. costatum* improved differentiation of NO_3 -utilizing from NH_4 -utilizing cells and is recommended for studies monitoring N-source dependent processes. The titer of the NR peptide epitope Ig was insufficient to overcome loss of Ig during the pre-absorption phase.

During the simulated upwelling experiment, immunolabeling by NR subunit antibodies pre-absorbed to NH_4 -grown *S. costatum* resolved low levels of NR protein under low f -ratio conditions and the initial and instantaneous increase in cellular NR abundance upon the shift to high f -ratio conditions (Fig. 3). Such resolution was not obtained by Western Blot densitometry (6). The low-level NR abundance revealed by immunocytometry was linked to extremely low but measurable NR activity (NRA). Again, these results may result from minor amounts of NO_3 in the Monterey Bay seawater used for culture preparation or reflect low constitutive NR levels that have been demonstrated earlier for this species (17). Non-specific binding can account for only a part of this low fluorescence signal since all presented results were corrected for non-specific binding of the secondary antibody, FITC-labeled goat-anti-rabbit IgG, and non-specific fluorescence signals of the applied anti-NR probe were only about 10 relative units.

The fast increase in NR abundance upon NO_3 addition has been demonstrated previously in *S. costatum* and assigned to the initiation of NR transcripts (17), and similar results are reported for the marine diatom *Thalassiosira weissfloggii* (18). After 48 hrs, NR protein leveled into a new physiological balance. Although the scatter in the data is quite high and temporal resolution too low to resolve diel patterns, it appears that NR abundance was

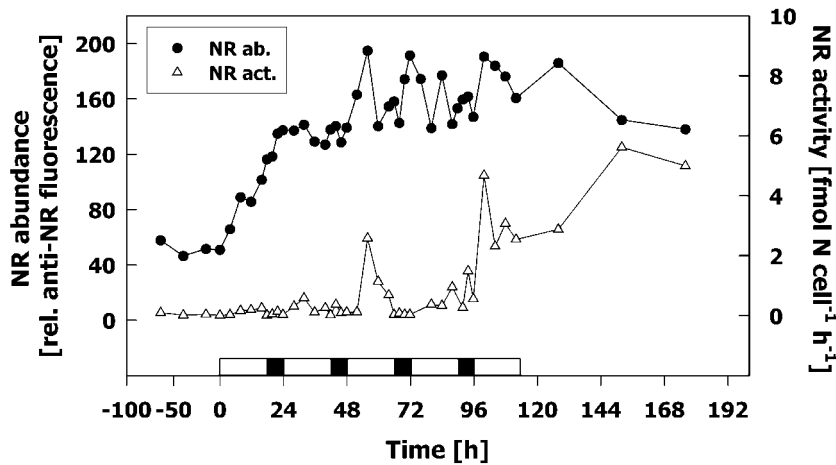


FIG. 3. Temporal changes of cellular NR protein abundance (NR ab., mean relative fluorescence units of anti-NR) and NR activity (NR act., $\text{fmol N cell}^{-1} \text{h}^{-1}$) during the upwelling simulation chemostat experiment. Nitrogen supply was changed from NH_4 to NO_3 at $t=0$, light/dark cycle is indicated during the first 114 hrs after nutrient shift when more than one daily sampling was performed.

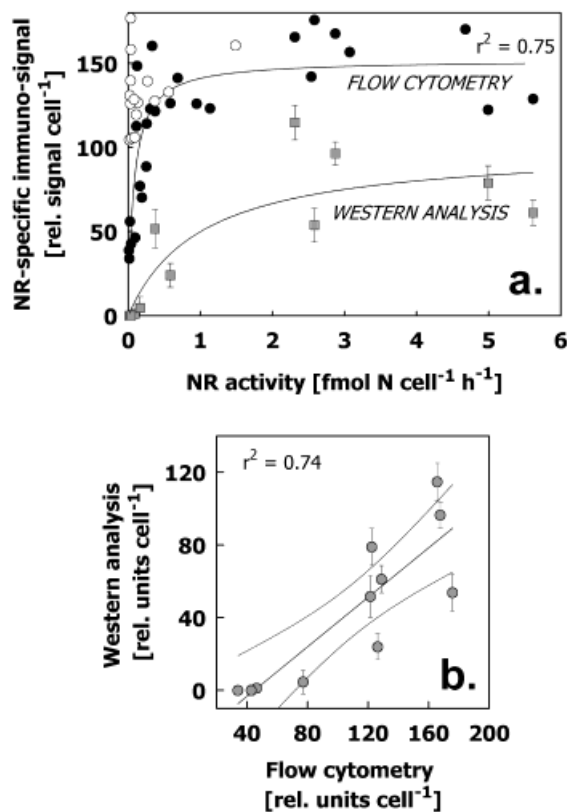


FIG. 4. a: Relation of NR protein abundance derived from densitometry of Western Blots and flow cytometry (both relative units) to NR activity ($\text{fmol N cell}^{-1} \text{h}^{-1}$). Filled circles = cytometry, light-phase samples; hollow circles = cytometry, dark-phase samples; squares = Western analysis of mid-day samples; b: relation between NR abundance (relative units) derived from densitometry of Western Blots and flow cytometry for mid-day samples ($r^2=0.74$, $P < 0.001$).

higher in the light than during the dark periods. This result corresponds to an earlier short-term nitrate-pulse experiment with *S. costatum* in which maximum NR abundance seemed to occur towards the end of the light cycle (17). The marine dinoflagellate *Gonyaulax poly-*

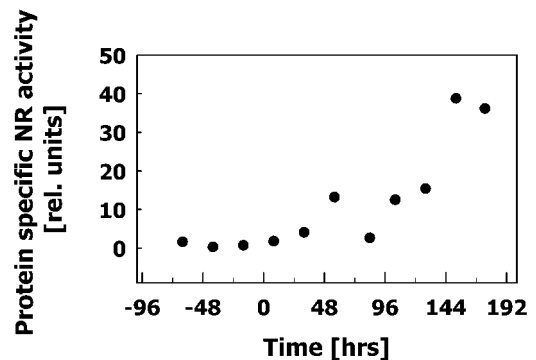


FIG. 5. Protein specific NR activity (NRA/NR ab. $\times 1000$; relative units) during the upwelling simulation chemostat experiment, mid-day samples only.

edra was also shown to exhibit a diel maximum NR abundance at mid-day, as revealed by immunogold labeling (19).

Detection of NR protein abundance by flow cytometry showed good agreement with densitometric analysis of western blots (Fig. 4b), and both methods exhibit a hyperbolic relationship to enzymatic assay of NR activity (NRA) in the light (Fig. 4a). Maximum NRA occurred during mid-light cycle (Fig. 3) as shown previously for natural diatom populations, *S. costatum* and *Thalassiosira weissflogii*, and the rhodophyte *Gracilaria tenuistipitata* (17, 18, 20, 21). This is consistent with the observed induction of NRA by light and repression in the dark (6, 17, 22). Therefore, no relation exists between NR protein abundance and NRA in dark-phase samples (Fig. 4a).

The hyperbolic relation of NR protein to NRA in light-phase samples is related to the less pronounced initial increase in NRA as compared to NR abundance (Fig. 3). The data suggest that the shift in f -ratio and nitrogen supply rate initiated NR synthesis, but the weak increase in NRA immediately after the shift might be related to activation of low NR protein contents already present during NH_4 growth. A strong increase in NRA occurred only after 2 days when NR

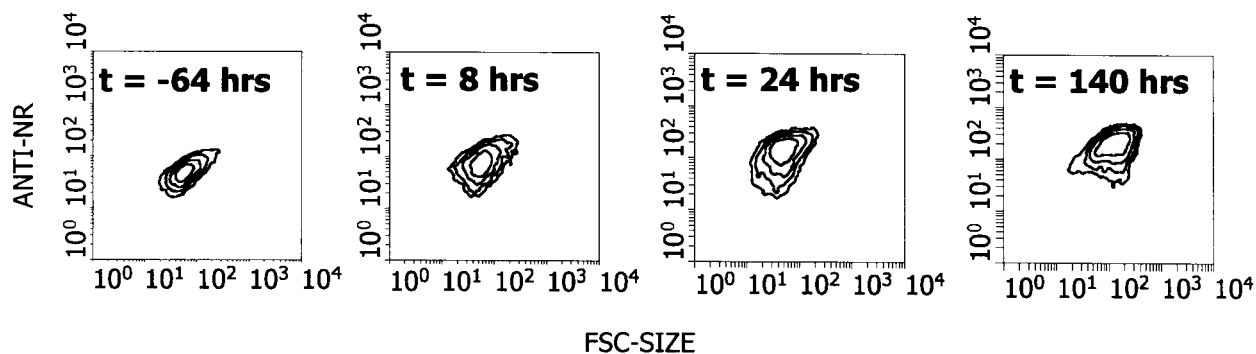


Fig. 6. Forward Angle Light Scatter versus anti-NR fluorescence at different times during the upwelling simulation experiment.

abundance had reached a new and higher “steady state”. This pattern points towards non-biosynthetic effects on NRA regulation consistent with the high degree of post-translational control of this enzyme known for *S. costatum* (17). As a consequence, protein-specific NRA increased 2 d after the nitrogen shift (Fig. 5).

The present NR antiserum does not differentiate active from inactive forms of NR protein, and activity of NR protein varies along physiological adaptation processes. Differentiation of active and inactive NR by the applied antiserum was not expected since specific Ig to target the activation sites (phosphorylation, co-factor binding, Fe-heme) would have to be designed for this task. Single cell, flow cytometric analysis of NR immunolabeling did, however, provide improved sensitivity for NR detection under conditions of low NRA, indicating that this technique is particularly valuable for monitoring early events during the induction of nitrate assimilatory capacity. Additionally, this assay provides strong signal discrimination between phytoplankton acclimated to NH_4 -supported versus NO_3 -supported growth. Flow cytometry provides the direct demonstration of population wide response to higher f -ratio and nitrogen supply rate that cannot be observed by test tube or filter paper measured induction of NR. Two-parameter-plots of Forward Angle Light Scatter (FSC) as a relative measure for cell size versus NR immunofluorescence suggest that all cells accumulated NR protein during the 24 hrs induction phase, followed by volumetric growth of the induced cells: At all sampling intervals, no high/low NR subpopulations were discernible as would have resulted from higher NR abundance in some but not all cells, but the culture always provided a picture of one homogeneous population (Fig. 6).

Field application is limited, however, by the restricted cross-reactivity of the NR antibody at hand. The polyclonal *S. costatum* NR antiserum showed positive immunolabeling in other marine diatoms (*Thalassiosira pseudonana*, *Phaeodactylum tricorutum*) but not in non-diatom species such as *Amphidinium carterae*, *Emiliania huxleyi*, *Isochrysis galbana*, *Dunaliella tertiolecta*, and *Synechococcus* sp. (6); it, thus, appears to be specific to diatoms. Antigenicity of nitrate reductases from different phytoplankton species seems divergent (11, 18) and despite

homologous amino acid domains corresponding to redox centers the overall similarity in amino acid sequences from different plant and fungal NR is less than 50% (23). There is evidence that NR from different algal classes are diverse and distinct in terms of biochemical characteristics and regulatory features (6, 7, 8, 11). These diversities might be related to the fact that diatoms present an evolutionary lineage distinct from that leading to land plants as documented by rDNA sequence comparison (24).

Polyclonal antibodies raised against squash NR showed fair cross-reactivity with several dinoflagellates, although this study may have been biased by non-specific binding (3). NR antibodies specific to dinoflagellates (25) may extend applications. Further antisera for species of interest in specific study areas or specific to other algal classes are to be developed and more taxonomically universe probes established for routine field application with diverse and complex phytoplankton communities. The generation of immunoprobe against widely conserved peptide sequence domains offers one approach for generic immunoassays (26). However, the observation that Ig pools targeting single epitopes may not yield sufficient signal for detection of low abundance targets, such as NR, suggests that this approach may have limited application. Still the present study demonstrates that the coupling of flow cytometry with immunological techniques can be used to assess nitrogen nutrition in phytoplankton and offers new insights into the study of nitrogen pathways.

LITERATURE CITED

1. Dugdale RC, Goering JJ. Uptake of new and regenerated forms of nitrogen in primary productivity. *Limnol Oceanogr* 1967;12:196-206.
2. Eppley RW, Peterson BJ. Particulate organic matter flux and planktonic new production in the deep ocean. *Nature* 1979;28:677-680.
3. Balch WM, Yentsch CM, Reguera B, Campbell W. Examining nitrate reductase by phytoplankton with an immunoassay. In: Yentsch CM, Mague FC, Horan PK, eds. *Immunochemical approaches to coastal, estuarine and oceanographic questions. Lecture notes on coastal and estuarine studies*. New York: Springer; 1988. p 263-276.
4. Beevers L, Hagman RH. Nitrate and nitrite reduction. In: Stumph PK, Conn EE, Mifflin BJ, eds. *The biochemistry in plants, a comprehensive treatise*, vol. 5: amino acids and derivatives. New York: Academic Press; 1980. p 115-168.
5. Solomonson LP, Barber MJ. Assimilatory nitrate reductase: functional properties and regulation. *Annu Rev Plant Physiol Plant Mol Biol* 1990;41:225-253.
6. Gao Y. Nitrate assimilation in the marine diatom *Skeletonema costatum*.

- tum* (Bacillariophyceae): Biochemical characterization and environmental regulation. Ph.D. thesis, University of Southern California. Los Angeles; 1997;211 p.
7. Berges JA. Algal nitrate reductases. *Eur J Phycol* 1997;32:3-8.
 8. Berges JA, Harrison PJ. Nitrate reductase activity quantitatively predicts the rate of nitrate incorporation under steady state light limitation: a revised assay and characterization of the enzyme in three species of marine phytoplankton. *Limnol Oceanogr* 1995;40:82-93.
 9. Berges JA, Harrison PJ. Relationships between nitrate reductase activity and rates of growth and nitrate incorporation under steady-state light or nitrate limitation in the marine diatom *Thalassiosira pseudonana* (Bacillariophyceae). *J Phycol* 1995;31:85-95.
 10. Joseph L, Villareal TA. Nitrate reductase activity as a measure of nitrogen incorporation in *Rhizosolenia formosa* (H. Peragallo): internal nitrate and diel effects. *J Exp Mar Biol Ecol* 1998;229:159-176.
 11. Gao Y, Smith J, Alberte RS. Nitrate reductase from the marine diatom *Skeletonema costatum*. *Plant Physiol* 1993;103:1437-1445.
 12. Guillard RRL, Kilham P. The ecology of marine planktonic diatoms. In: Werner D, ed. *The biology of diatoms*. Berkeley: University of California Press; 1977. p. 372-469.
 13. Round FE, Crawford RM, Mann DG. *The diatoms: biology and morphology of the genera*. Cambridge: University Press; 1990.
 14. Guillard RRL, Ryther JH. Studies of marine planktonic diatoms. I. *Cyclotella nana* Hustedt and *Detonula confervacea* Cleve. *Can J Microbiol* 1962;8:229-239.
 15. Guillard RRL. Culture of phytoplankton for feeding marine invertebrates. In: Smith WL, Chanley MH, eds. *Culture of marine invertebrate animals*. New York: Plenum Press; 1975. p. 26-60.
 16. Timmons TM, Dunbar BS. Protein blotting and immunodetection. In: Deutscher MP, ed. *Guide to protein purification*. San Diego: Academic Press; 1990. p. 679-688.
 17. Smith GJ, Zimmerman RC, Alberte RS. Molecular and physiological responses of diatoms to variable levels of irradiance and nitrogen availability: growth of *Skeletonema costatum* in simulated upwelling condition. *Limnol Oceanogr* 1992;37:989-1007.
 18. Vergara JJ, Berges JA, Falkowski PG. Diel periodicity in nitrate reductase activity and protein levels in the marine diatom *Thalassiosira weissfloggii* (Bacillariophyceae). *J Phycol* 1998;34:952-961.
 19. Fritz L, Stringher CG, Colepicolo P. Imaging oscillations in *Gonyaulax*: a chloroplast rhythm of nitrate reductase visualized by immunocytochemistry. *Braz J Med Biol Res* 1996;29:111-117.
 20. Berges JA, Cochlan WP, Harrison PJ. Laboratory and field responses of algal nitrate reductase to diel periodicity in irradiance, nitrate exhaustion, and the presence of ammonium. *Mar Ecol Prog Ser* 1995;124:259-269.
 21. Lopes PF, Oliveira MC, Colepicolo P. Diurnal fluctuation of nitrate reductase activity in the marine red alga *Gracilaria tenuistipitata* (Rhodophyta). *J Phycol* 1997;33:225-231.
 22. Gao Y, Smith GJ, Alberte RS. Light regulation of nitrate reductase in *Ulva fenestrata* (Chlorophyceae). I. Influence of light regimes on nitrate reductase activity. *Mar Biol* 1992;112:691-696.
 23. Campbell WH, Kinghorn JR. Functional domains of assimilatory nitrate reductases and nitrite reductases. *Trends Biochem Sci* 1990;15:315-319.
 24. Gunderson JH, Elwood H, Ingold A, Kindle K, Sogin ML. Phylogenetic relationships between chlorophytes, chrysophytes, and oomycetes. *Proc Natl Acad Sci USA* 1987;84:5823-5827.
 25. Fritz L, Stringher CG, Colepicolo P. Immunolocalization of nitrate reductase in the marine dinoflagellate *Gonyaulax polyedra* (Pyrrophyta). *J Phycol* 1996;32:632-637.
 26. Smith GJ, Gao Y, Alberte RS. Immunological probes of new production: universal and taxon-specific markers for nitrate reductase in marine algae. *EOS* 1996;76:62.